JOURNAL OF MATERIALS SCIENCE 11 (1976) 417–424

Environmental crazing and intrinsic tensile deformation in polymethylmethacrylate

Part 1 *Mechanical behaviour*

YASUFUMI IMAI*, NORMAN BROWN
Department of Metallurgy and Materials Science and Laboratory for Research on the Structure of Matter, University of Pennsylvania, Philadelphia, USA

The tensile stress–strain behaviour of PMMA was measured from 77 to 350 K in He which provides an inert environment and in N_2, Ar, O_2, CO_2, and water which cause crazing. The effect of the partial pressure of the crazing agent on the tensile properties was measured. It was found that the ratio of the tensile strength in a crazing environment to that in an inert environment depended on temperature and pressure as follows: $\sigma_c/\sigma_i = \{P \exp(Q/RT)/P^*\}^{-0.13}$ where P^* and Q depend on the crazing agent. The critical temperature and pressure which determine when a gas ceases to produce an environmental effect on the tensile strength is given by the condition that $P \exp(Q/RT) < P^*$. Above 273 K the intrinsic deformation changed from brittle fracture to a combination of intrinsic crazing and shear.

1. Introduction

Parrish and Brown [1] first showed that N_2 and Ar cause crazing in linear polymers at low temperatures. All investigations support the general idea that any gas with the possible exception of helium can modify the tensile strength of every linear polymer if the temperature and pressure are properly chosen and that the gases act as a crazing agent. Both amorphous and crystalline polymers exhibit the same behaviour except crazes are more difficult to observe in crystalline polymers as shown by Brown and Fischer [2] in PTFE.

Brown and Imai [3, 4] delineated the critical conditions of temperature and pressure whereby N_2, Ar, or O_2 causes crazing in polycarbonate. If the pressure is too low for a given temperature or if the temperature is too high for a given pressure, then these gases are not effective and the intrinsic behaviour, as compared with the environmental effect, can be observed. The intrinsic behaviour can be observed in vacuum or helium. Olf and Peterlin [5] studied crystalline and non-crystalline polypropylene under one atmosphere of N_2, Ar, O_2, CO_2 or He from 77 K to above 373 K and determined the critical temperature above which each gas ceased to be crazing agent. They also observed intrinsic crazing in the inert environment of He. Hiltner *et al.* [6] observed polyethylene terephthalate in N_2 and He from 4.2 K to about 300 K. They found that the environmental effects of N_2 ceased above about 150 K, and they reported no effects from He. All experiments to date indicate that all gases, with the possible exception of He, have the potential to cause any linear polymer to craze and/or to affect its tensile strength.

It is generally agreed that these gases plasticize and reduce the surface energy of a microvolume of material at the tip of the craze. If a critical amount of sorption is required for crazing, then too low a pressure or too high a temperature would desorb the gas so that crazing would not occur. Theory and experiments [4, 5] indicate that the effective temperature range of a particular gas would depend on its boiling point and the interaction energy between the gas and the polymer. Instead of considering separately the critical temperature and pressure that will just cause crazing, it is better to think in terms of a critical amount of sorbed gas being necessary.

---

[*] Permanent address: Nagasaki University, Nagasaki, Japan.

© *1976 Chapman and Hall Ltd. Printed in Great Britain.*

In this investigation the effects of N_2, Ar, O_2, CO_2 and water on the tensile properties of PMMA substitute were observed from 77 K to about 370 K and the partial pressure of the gas was varied from 0 to 1 atm. The relationship between the craze yield point and the intrinsic tensile strength, the pressure and the temperature of the gas was similar to that found for PC [4]. The craze yield point is proportional to the intrinsic tensile strength and is a function of the concentration of sorbed gas. In this paper the mechanical behaviour is presented and in Part 2, the difference in the structure of environmental and intrinsic crazing is presented and a microscopic model for crazing is given. The results of this investigation reinforce the idea that almost every gas or liquid under the proper temperature and pressure has the capacity to cause any thermoplastic to craze with helium being the possible exception.

2. Experimental

The PMMA was commercial Plexi-glass (G) and in the form of 0.6 mm thick sheet. The tensile specimens were cut with a high speed milling machine in the shape of 5 mm width and 12.7 mm uniform gauge length.

The desired pressure of a crazing agent gas was obtained as a partial pressure of the mixture with He gas; the total pressure was always 1.0 atm. The flow rates of both crazing gas and helium were precisely controlled with a manometer-controlled flow meter during the course of the experiment so that the partial pressure of the crazing gas was held constant within ± 1%. The purity of the He, N_2 and Ar was within 99.99%, O_2 was 99.6%, and CO_2 was 99.5% pure. The water was distilled.

The temperature of the specimen and the surrounding gas was controlled by a cold bath and an electric heater. Three thermocouples along the gauge length were used to measure the temperature of the specimen and also the temperature gradient. It is estimated that the temperature gradient was within $2^\circ \mathrm{C\,cm^{-1}}$ and hence, the temperature is known within $\pm 1^\circ$ C. The tempeature fluctuation was kept constant within $\pm 0.5^\circ$ C during the course of the testing. Thermal equilibrium was also detectable by recording load associated with the thermal contraction and elongation. The pre-tension load was kept constant around 3 to 5% of the fracture load.

The stress–strain data were obtained with an Instron machine. The cross-head speed for all experiments was $0.25\ \mathrm{mm\,min^{-1}}$. The strain was calculated from the cross-head displacement and an effective gauge length of 25 mm. The error in stress is primarily associated with the un-uniformity of thickness of specimens and is about ± 1.5 MPa.

3. Results

3.1. Stress–strain curves at various pressures

Fig. 1a to c shows the stress–strain curves in N_2, Ar and CO_2 at various pressures and a fixed temperature. Crazes were observed in all these tests except at $P = 0$ which corresponds to pure He. P is defined as the partial pressure of the crazing agent. At $P = 1$ atm a craze yield point was observed in all the gases, but as the pressure decreased the specimens tended to fracture before the yield point. In all cases the tensile strength increased as P decreased. Young's modulus is independent of P. The stress–strain curves in O_2 were similar to those for N_2 and Ar except that the temperature of observation was slightly higher.

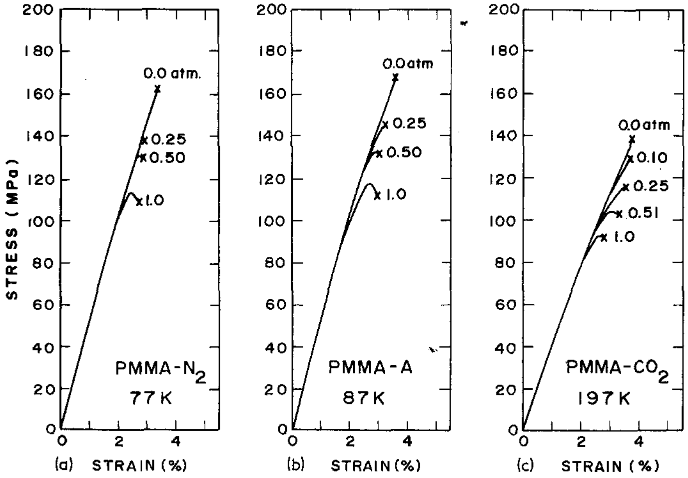

Figure 1 Stress–strain curves at various partial pressures (a) in N_2 at 77 K, (b) in Ar at 87 K, (c) in CO_2 at 197 K.

3.2. Intrinsic stress–strain curves from 77 to 352 K

Fig. 2a shows the stress–strain curves at $P = 0$. In an inert environment, the tensile strength decreases uniformly with increasing temperature as does Young's modulus. Curve GHJ in Fig. 3 shows how the tensile strength changes with T. The tensile strength extrapolates to zero at $T \simeq T_g$.

Below about 240 K the tensile strength corresponds to the brittle fracture stress. Above 240 K the ductility gradually increases until a shear yield point was observed at about 283 K. Fracture strain versus T is shown in Fig. 4. Once shear yielding occurs the specimen draws and very large strains are observed. At room temperature the ductility varied from about 12 to above 20% depending on the time that the specimen was exposed to the ambient environment of the laboratory after the sticky protective paper was removed.

Below 283 K no evidence of deformation, except for the fracture surface, was observed. Above 283 K intrinsic crazing and deformation bands became more evident with increasing temperature as the specimens exhibited greater ductility. The intrinsic crazes were generally shorter

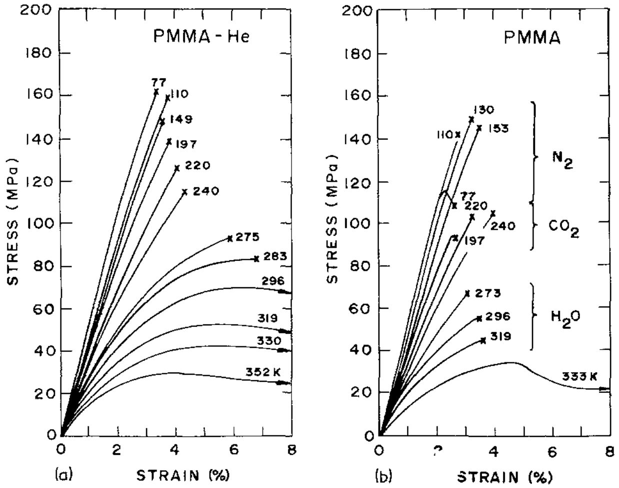

Figure 2 Stress–strain curves at various temperatures (a) in He at 1 atm, (b) in pure N_2, CO_2, and water at 1 atm.

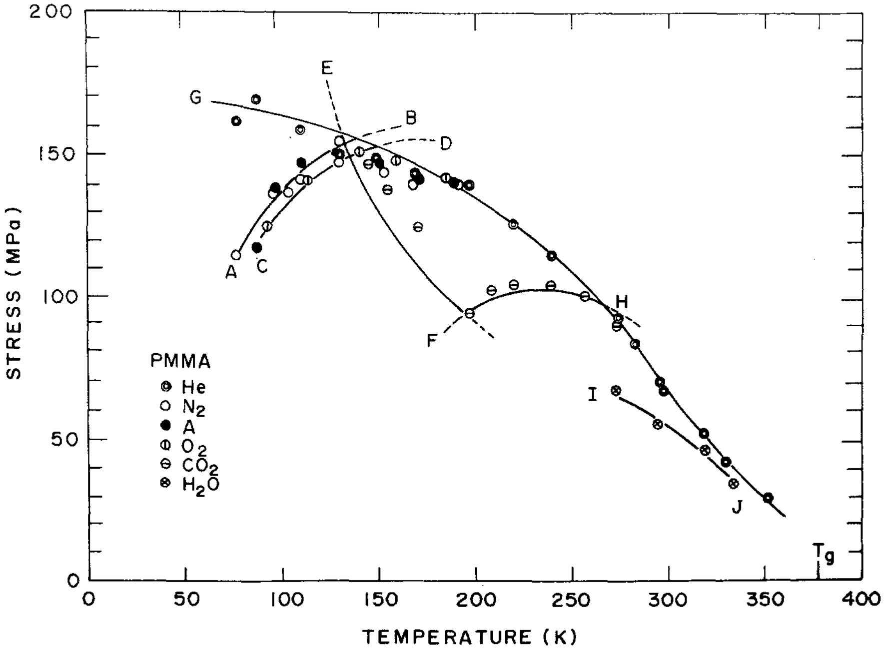

Figure 3 Brittle fracture stress or shear yield point versus T for $P = 1$ atm in various environments. GHF in He, AB in N_2 and Ar, CD in O_2, FH in CO_2 gas, FE in CO_2 vapour in equilibirum with solid CO_2, and IJ in water.

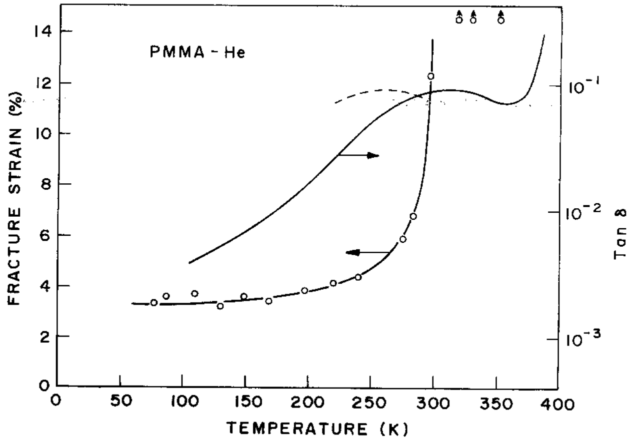

Figure 4 Strain at fracture versus T in He. Internal friction versus T.

and more uniformly distributed over the surface of the specimen when compared to the environmental crazes which were generally longer and tended to initiate at the edge of the specimen.

3.3. Stress–strain behaviour in N_2, Ar, and O_2 at different temperatures

The stress–strain curves in N_2 at $P = 1$ atm are shown in Fig. 2b. Crazes were observed from 77 to 140 K, but a craze yield point was observed only at the lower temperatures; as the temperature increased, the specimen craze-fractured before it craze-yielded. The Ar and O_2 behaved similarly to N_2 except O_2 exhibited crazes up to about 160 K. The variation of tensile strength with T at $P = 1$ atm is shown in Fig. 3 where the branch AB is for N_2 and Ar and CD is for O_2. No appreciable discontinuity in behaviour was observed between the gas and the liquid in the region of the boiling point.

3.4. Stress–strain behaviour in CO_2

The stress–strain curves in CO_2 at various temperatures at $P = 1$ atm is shown in Fig. 2b. In CO_2 crazing was not observed above about 250 K. The tensile strength as a function of T at $P = 1$ atm goes through a maximum as shown by the branch FH in Fig. 3. The sublimation temperature of $P = 1$ atm is 195 K. Below 195 K the vapour pressure of CO_2 decreases rapidly with temperature and, therefore, the tensile strength in the environment of solid CO_2 increases along the curve FE in Fig. 3. When the vapour pressure became too low at about 140 K, crazing stopped and simple brittle fracture was observed. The vapour pressure of CO_2 at 140 K is about 2×10^{-3} atm.

3.5. Stress–strain behaviour in water

The stress–strain curves in ordinary distilled water from 273 to 333 K are shown in Fig. 2b. Long environmental crazes were observed in water. Up to 319 K craze fracture occurred and the ductility was sharply reduced as compared to the intrinsic stress–strain curves (Fig. 2a) in the same temperature range. At 333 K a yield point was observed and the specimen exhibited long environmental crazes, profuse short intrinsic crazes, and deformation bands altogether on the same specimen. In Fig. 3 the branch IJ shows the tensile strength in water as compared to the intrinsic shear yield point which follows the curve HJ.

4. Synthesis

4.1. Synthesis of the pressure and temperature effects of the environment on the tensile strength

The effect of P and T on the craze yield point of polycarbonate in N_2, Ar, and O_2 has been described by Brown and Imai [4] in terms of the following equation:

$$\sigma_c/\sigma_s = \{P \exp(Q/RT)/P^*\}^{-0.08} \qquad (1)$$

where σ_s is the intrinsic shear yield point and Q and P^* are constants which depends on the particular gaseous environment. Theories of crazing [7–9] agree with the experimental statement contained in Equation 1 which states that the craze yield point should be proportional to the intrinsic shear yield point of the bulk polymer. In the case of PMMA at low temperatures, the environmental tensile strength is either a craze fracture stress or a craze yield stress and will be designated as σ_c. It is now being suggested that σ_c is proportional to the

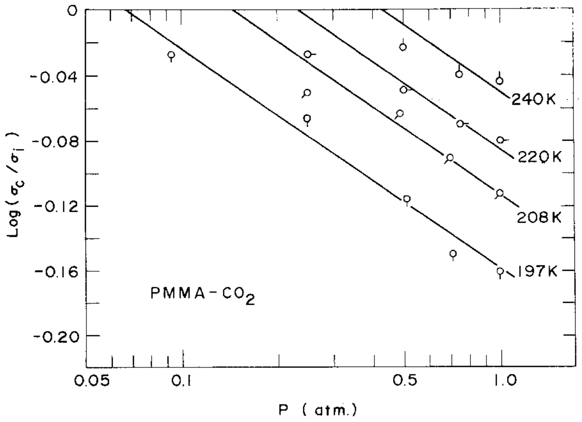

Figure 5 Log ratio of tensile strength in CO_2 to tensile strength in He versus log partial pressure of CO_2 at various temperatures.

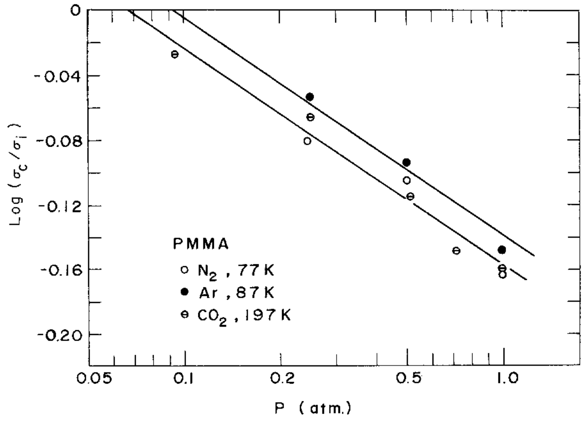

Figure 6 Same as Fig. 5 for N_2, Ar, and CO_2 environments.

intrinsic tensile strength, σ_i. In accordance with this suggestion log σ_c/σ_i was plotted against log P for a fixed T, and the results are shown in Fig. 5 for CO_2. The linear relationship in Fig. 5 corresponds to Equation 1 except that the exponent is -0.13 for PMMA instead of -0.08 for PC. Log σ_c/σ_i versus log P is plotted for N_2, Ar, and CO_2 in Fig. 6 and the combined data corresponds to a slope of -0.13. These results suggest that for all the environments and a given polymer the slope of log σ_c/σ_i versus log P may be a constant, which for PMMA equals -0.13.

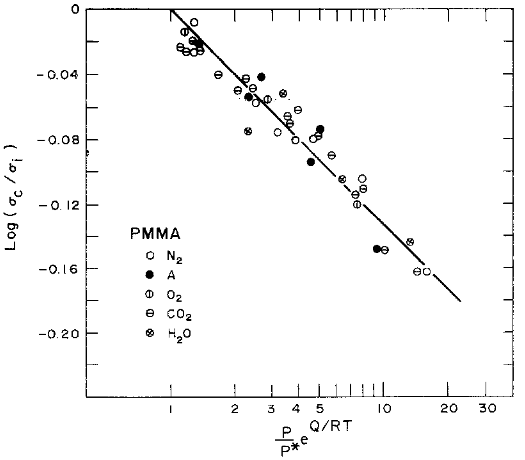

Figure 7 Plot showing that $\sigma_c/\sigma_i = \{P \exp(Q/RT)/P^*\}^{-0.13}$ using the values of P^* and Q given in Table I.

The effect of temperature was obtained by plotting log σ_c/σ_i versus $1/T$ for a constant P. These plots were sufficiently linear with a slope that depended on the particular environment. Thus, all the data for PMMA could be represented by the following equation.

$$\sigma_c/\sigma_i = \{P \exp(Q/RT)/P^*\}^{-0.13} \qquad (2)$$

as shown in Fig. 7. Table I gives the values P^* and Q corresponding to each environment. The column T_{cr} in Table I corresponds to the critical temperature at $P = 1$ atm above which crazing stops and the intrinsic strength is observed. T_{cr} was calculated from Equation 2 and the observed values of T_{cr} were based on the microscopic observations of crazing. Note that Q increases with the boiling point.

4.2. The *P–T* deformation diagram

In P–T space, the deformation of polymers can be divided into an intrinsic domain and an environmentally controlled domain. Each polymer and a particular gas has its P–T deformation diagram. The boundary between the intrinsic deformation domain and the environmentally controlled domain is obtained from Equation 2 by setting $\sigma_c/\sigma_i = 1$ so that the critical combination of temperature,

TABLE I Parameters in Equation 2

Environment	P^*(atm)	Q(kcal mol^{-1})	T_{cr}(K)(calc)	T_{cr}(obs)
N_2	30	0.94	139	140
Ar	40	1.02	139	140
O_2	34	1.03	146	160
CO_2	2160	4.05	265	250
Water	1200	5.25	373	–

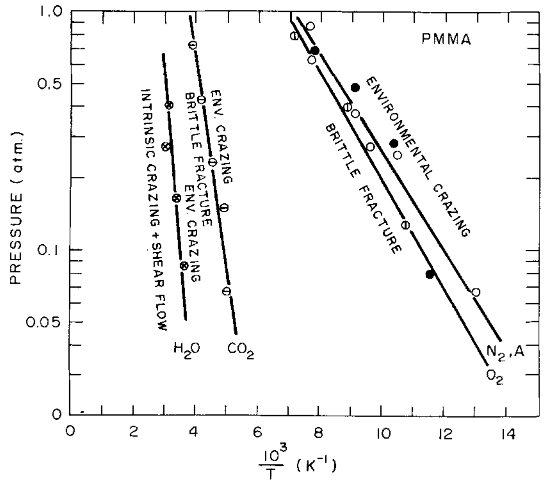

Figure 8 P–T deformation diagram showing the boundary between the intrinsic and crazing domains for each of the environments, N_2, Ar, O_2, CO_2 and water.

T_{cr}, and pressure, P_{cr}, is given by

$$P^* = P_{cr} e^{Q/RT_{cr}} \quad (3)$$

Fig. 8 gives the P–T deformation diagrams for PMMA in N_2, Ar, O_2, CO_2, and water. Further experiments are required to extend the range of the domain boundaries. At very high pressures, the stress effect per se would add to the environmental effect so that Equation 3 would not be adequate to define the domain boundary. Also at very high hydrostatic pressures crazing can be completely suppressed by the stress no matter what is the temperature or the environment.

5. Discussion

5.1. The intrinsic tensile strength and Young's modulus

The intrinsic tensile strength may be a brittle fracture stress, σ_b, or a shear yield point, σ_s, in an inert environment. The values of σ_b and σ_s as a function of T are given by the curves GH and HJ respectively in Fig. 3. In this paper for the first time, the intrinsic tensile strength of PMMA at low temperatures is fully displayed because practically all previous work was done in an active environment such as air or liquid N_2.

It was pointed out by Brown [10] that the yield point of a polymer is related to its modulus and that for all polymers the ratio of yield point to modulus lies in the range of about 1/30 to 1/60. This rule was also obeyed under the hydrostatic pressure which changes the yield point and modulus proportionately. If the ratio of tensile strength to Young's modulus is about 1/30, then one can conclude that the tensile strength is very close to its maximum theoretical value [11]. It is very surprising that a solid as imperfect as a polymer should always exhibit a tensile strength which approaches the ideal strength whereas metals usually have a much lower tensile strength in comparison to the modulus.

The ratios of the intrinsic tensile strengths to Young's modulus, σ_b/E and σ_s/E, are plotted in Fig. 9 versus T. All the data fall in the range of 1/30 to 1/50. However the σ_b/E ratio is essentially independent of T and σ_s/E increases with decreasing T. The scatter in σ_b/E is expected because the brittle fracture strength is sensitive to defects in the material and those produced when the specimen was machined. The decrease in σ_s/E with increasing T is attributed to the fact that the shear yield strength is lowered more by thermal activation than is the modulus. Thermal activation is reflected in the dependence of shear yield point on the strain–rate whereas the modulus is much less effected by strain–rate.

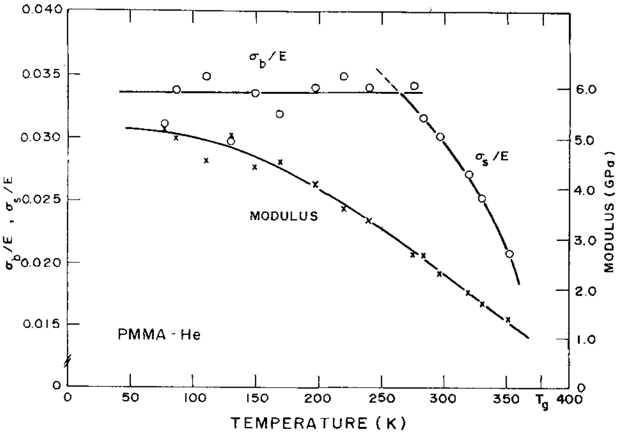

Figure 9 Young's modulus versus T. Ratio of intrinsic brittle fracture stress to Young's modulus, (σ_b/E) and ratio of intrinsic shear yield point to Young's modulus, (σ_s/E), each versus T.

5.2. Intrinsic ductility

The fracture strain versus T is shown in Fig. 4. The rapid increase in ductility with T is associated with the β relaxation process. The internal friction versus T at 1 Hz is also shown in Fig. 4 with the β peak occurring at 310 K. For the strain-rate used in these tensile tests, it is estimated that the corresponding frequency for comparison with the internal friction data should be about 10^{-2} Hz. At 10^{-2} Hz, the β peak occurs at about 260 K which is just about where the ductility begins to increase very rapidly. The β peak also corresponds to the intersection of the σ_b/E and σ_s/E curves in Fig. 9. The ductility begins to increase at about 200 K because the β relaxation becomes significant above 200 K. Hiltner *et al.* [6] have also emphasized the dependence of the ductile–brittle transition on the molecular relaxation processes.

The nature of the intrinsic mechanical properties may be summarized as follows: (1) the tensile strength is 1/30 to 1/50 times Young's modulus and (2) the ductility as reflected by the brittle to ductile transition is related to the occurrence of the β relaxation. In the past, the true nature of the ductile–brittle transition was often obscured by the environmental effects.

5.3. The environmental effect

The physical explanation of Equations 1 and 2 is based on the idea that the concentration of sorbed crazing agent in a microvolume of polymer at the edge of the craze is most important. Since the absorption [12] or adsorption [13] of gas in a polymer is described in general by a function of $Pe^{Q/RT}$, Equation 2 can be interpreted as follows

$$\sigma_c/\sigma_s = [S/S^*]^{-0.13}$$

where S is the concentration of sorbed gas and S^* is the critical concentration which will produce crazing. The significance of the exponent −0.13 is not understood, but from work on PC and PCTFE, it appears that this exponent depends strongly on the polymer. The sorption of a gas in a polymer is likely to increase with the boiling point of the gas. The enthalpy for sorption should in some way be related to the Q values in Table I. Note that Q generally increases with the boiling point but is not simply proportional to it.

The tensile strength as a function of the temperature tends to go through a maximum for a fixed pressure of the environmental gas since: (1) σ_c tends to decrease with increasing T because σ_i does and (2) σ_c tend to increase with increasing T because sorption decreases. The maximum in σ_c with T will not always be observed because crazing ceases when $\sigma_c > \sigma_i$.

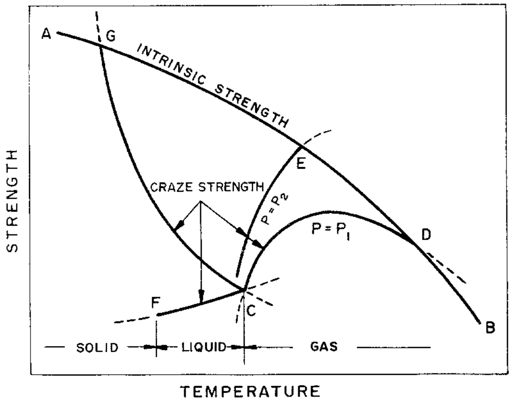

Figure 10 Schematic diagram showing the general effect of a crazing agent on the tensile strength as a function of temperature. AGDB is for an inert environment. CD and CE corresponds to the gas at pressures P_1 and P_2 with $P_1 > P_2$. CF is for the polymer in contact with the liquid. CG is for the polymer in contact with the vapour when the vapour is in equilibrium with the solid or liquid.

The general effect of a crazing agent in the gas, liquid, and solid state can be described by Fig. 10 where AB is the curve of intrinsic strength versus T. The curve CD is the strength of a gaseous crazing agent at a pressure P_1 and CE is for the gas at a lower pressure, P_2. CF is the curve when the polymer is immersed in a liquid. There are no data to indicate whether its slope is positive or negative for the liquid. The existing data do not indicate that a discontinuity exists between the liquid and gaseous states near the boiling point. One important difference between the gas and liquid state is that the craze velocity in a liquid may be governed by diffusion through the craze as suggested by Marshall *et al.* [14]; whereas in a gas the craze velocity is controlled by the diffusion into the polymer itself at the edge of the craze as suggested by Brown [15]. The effect of the vapour of a solid or a liquid as a crazing agent depends on the vapour pressure. The curve CG (Fig. 10) represents the tensile strength versus T in the presence of a vapour which is in equilibirum with a solid or a liquid. The tensile strength rises as the vapour pressure decreased with decreasing temperature. The curve FE in Fig. 3 was calculated using Equation 2 and the known dependence of the vapour pressure of solid CO_2 on T. The agreement between the experimental points and the theoretical curve is quite good.

In summary: it is suggested that almost any gas or liquid can be a crazing agent for any polymer if the gas or liquid can be sorbed by the polymer. The critical amount of sorption to produce crazing would depend on the temperature and pressure.

Acknowledgements

The work was primarily supported by the U.S. Army Research Office and partly by the National Science Foundation through the LRSM grant.

References

1. M. F. PARRISH and N. BROWN, *Nature* **237** (1972) 122.
2. S. FISCHER and N. BROWN, *J. Appl. Phys.* **44** (1973) 4322.
3. N. BROWN and Y. IMAI, *J. Polymer Sci. Letters* **13** (1975) 511.
4. N. BROWN and Y. IMAI, *J. Appl. Phys.* **48** (1975) 4130.
5. H. G. OLF and A. PETERLIN, *J. Polymer Sci.-Phys. Ed.* **12** (1974) 2209.
6. A. HILTNER, J. A. KASTELIC and E. BAER, "Advances in Polymer Science and Engineering", edited by K. D. Pae, D. R. Morrow, and Yu Chen (Plenum Press, New York, 1972) p. 335.
7. N. BROWN and S. FISCHER, *J. Polymer Sci.-Phys. Ed.* to be published.
8. A. S. ARGON, "Heterogeneities in Polymers", edited by B. Sedlacek and B. C. L. Weedon, (Butterworth, London, 1975).
9. E. H. ANDREWS and L. BEVAN, *Polymers* **13** (1972) 337.
10. N. BROWN, *Mat. Sci. Eng.* 8 (1971) 69.
11. A. KELLY, "Strong Solids", (Clarendon Press, Oxford, 1966).
12. J. H. HILDEBRAND and R. L. SCOTT, "The Solubility of Non-electrolytes", Dover Publications New York, 1964) p. 244.
13. S. J. GREGG, "The Surface Chemistry of Solids", 2nd Edn. (Rheinhold, New York, 1961).
14. C. P. MARSHALL, L. E. CULVER and J. G. WILLIAMS, *Proc. Roy. Soc. London* **A319** (1970) 165.
15. N. BROWN, *J. Polymer Sci.-Phys. Ed.* **11** (1973) 2099.

Received 9 July and accepted 29 July 1975.